

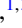



High-throughput predictions of two-dimensional dielectrics with first-principles calculations

Gege Du ^{1,*}, Chunhui Li ^{2,*}, Lei Shan ^{1,3,†} and Long Cheng ^{1,‡}

¹*School of Physics and Electronics, Hunan University, Changsha 410082, China*

²*School of Computational Science and Electronics, Hunan Institute of Engineering, Xiangtan 411104, China*

³*National Engineering Research Center of RVC, Hunan University, Changsha 410082, China*



(Received 12 September 2023; revised 18 October 2023; accepted 20 November 2023; published 7 December 2023)

Two-dimensional (2D) dielectrics play a crucial role in the miniaturization of transistors. An optimal 2D dielectric should have a significant out-of-plane dielectric constant and appropriate band alignments to achieve superior performance. However, 2D materials generally exhibit poor out-of-plane dielectric constant. In this paper, we have identified 11 2D materials from the Computational 2D Materials Database with out-of-plane dielectric constants above 5.0, surpassing those of conventional dielectrics, i.e., SiO₂, Al₂O₃, and BN. The band alignments show that ten monolayers SnNa₂H₆O₆, GeLi₂H₆O₆, HfNa₂H₆O₆, ZrNa₂H₆O₆, etc., are promising dielectrics when monolayer MoS₂/WS₂ serves as the channel. Moreover, four dielectrics have an out-of-plane dielectric constant that outperforms in-plane. This unusual feature indicates a stronger out-of-plane bond strength, resulting from the ionic bonds. We further provide a general guideline for quickly discovering high-performance dielectrics using structures and electronegativity tables.

DOI: [10.1103/PhysRevB.108.235409](https://doi.org/10.1103/PhysRevB.108.235409)

I. INTRODUCTION

As Moore's Law gradually loses its effectiveness, enhancing the performance of semiconductor chips becomes increasingly challenging. One solution is to introduce two-dimensional (2D) materials in manufacturing field-effect transistors (FETs), which are the basic building blocks of chips. 2D materials, i.e., monolayer MoS₂ and black phosphorene (BP), have already shown extensive application prospects in nanoelectronics [1–3]. In 2014, a nano-FET composed entirely of 2D materials for the source, gate, drain, and channel materials was fabricated [4]. Unfortunately, the performance of all the 2D FETs fabricated still cannot compete with the silicon-based FET [5,6]. The performance of a FET is influenced by various factors, such as the carrier mobility of the channel material, the contact resistance, the dielectric properties of the gate material, etc. [5,7]. Previous endeavors have been mainly devoted to discovering different channel materials and reducing contact resistance [5,7–9]. We have also conducted a comprehensive theoretical study on electron transport in 2D semiconductors and identified several high-mobility 2D semiconductors that could serve as channel materials [10–13].

By contrast, research on 2D gate dielectrics is relatively limited. Conventional FET devices often employ silicon dioxide (SiO₂), boron nitride (BN), or aluminum oxide (Al₂O₃) as gate materials [14–16]. However, the dielectric properties of these materials are not exceptionally high and achieving desired dielectric performance requires a relatively thick dielectric layer, typically on the order of tens of nanometers,

which is detrimental to the miniaturization of devices. Furthermore, integrating these dielectrics onto the surface of channel material involves complex processes. A feasible approach is to introduce 2D materials as gate dielectrics. This method not only reduces the thickness of the dielectric layer to less than a nanometer but could also simplify device fabrication by leveraging the nature of 2D materials through van der Waals (vdW) integration techniques [17–20].

A good 2D dielectric should have a large band gap (>3.0 eV), a significant out-of-plane dielectric constant $\epsilon_{o,\perp}^{2D}$, and an adequate electron affinity. Typically, $\epsilon_{o,\perp}^{2D}$ of 2D semiconductors is considerably small, making it difficult to identify suitable 2D dielectrics. Recently, Vandenberghe *et al.* [21] identified several potential candidates with high dielectric performance through first-principles calculations, such as LaOBr, LaOCl, and SrI₂. Hou *et al.* [22] have successfully fabricated a high-performance LaOCl gate dielectric. However, all these materials contain either lanthanide metals or rare-earth elements, rendering their fabrication costs significantly higher than materials such as SiO₂ and Al₂O₃. Therefore, it is desirable to search for new 2D dielectrics composed of cheap and earth-abundant elements.

In this study, 271 stable monolayers out of the 15733 materials with a band gap exceeding 3.0 eV were screened out from the Computational 2D Materials Database (C2DB) [23,24]. Their dielectric properties are then studied by using first-principles calculations. It is found that 11 candidates have $\epsilon_{o,\perp}^{2D} > 5.0$, rendering their potential as 2D dielectrics. Moreover, nine have both in-plane and out-of-plane dielectric constants larger than 5.0, and four have an out-of-plane dielectric constant that outperforms the in-plane dielectric constant. In addition, based on chemical bond analysis, we obtain a general rule to quickly access good dielectrics from structural properties and electronegativity of elements: searching for high $\epsilon_{o,\perp}^{2D}$ dielectrics is to find materials with bonds along

*These authors contributed equally to this work.

†Corresponding author: leishan@hnu.edu.cn

‡Corresponding author: lcheng@hnu.edu.cn

out-of-plane that are highly ionic, which means the atoms forming this bond have a large difference in electronegativity.

II. COMPUTATIONAL METHODS

All the first-principles calculations are carried out by using the Vienna *ab initio* Simulation Package (VASP) [25–27] with the projector augmented wave (PAW) potentials [28]. The exchange-correlation functional is in the form of Perdew-Burke-Ernzerhof (PBE) with generalized gradient approximation (GGA) [29,30]. The energy cutoff is set as 30% higher than recommended, and the k -point mesh is sampled by a separation of $0.03 \times 2\pi/\text{\AA}$. All the structures extracted from the C2DB are reoptimized with the force criterion less than 10^{-5} eV/\AA. The Heyd-Scuseria-Ernzerhof (HSE06) [31,32] method is adopted to predict band alignments and band gaps more reliably.

III. RESULTS AND DISCUSSION

Our selection procedure starts from the 15 733 monolayers in the C2DB, of which 2717 exhibit both high energetic and thermodynamic stability. A dielectric should first be a poor conductor, thus having a large enough band gap to preclude electrons from being excited from the valance band to the conduction band via thermal fluctuation. Therefore, we applied a band gap criterion $E_g > 3$ eV and screened 271 stable monolayers. Note that the band gap in C2DB is in the PBE level. The 3-eV criterion is to identify monolayers with a higher enough band gap after correcting for the PBE underestimation. It is found that those materials cannot be classified into several simple categories based on their lattice structure and space group. While considering the chemical composition, most monolayers are binary, ternary, and quaternary compounds, and 11 are five-membered compounds. Moreover, we found that most monolayers contain either hydrogen, oxygen, or both elements, which suggests that the potential high dielectric constant candidates also contain hydrogen and oxygen. In addition, the commonly used 2D dielectrics in nanotransistors, i.e., hexagonal BN [15], and the theoretically studied MgX_2 ($X = \text{Cl}, \text{Br}, \text{and I}$) and ZnX_2 ($X = \text{Br}, \text{I}$) monolayers [21] are also in the list (the complete list of the 271 monolayers are in the Supplemental Material [33]). The screening flow is indicated in Fig. 1(a).

We then studied the dielectric properties of the 271 monolayers, considering that three-dimensional (3D) periodic boundary conditions adopted in conventional *ab initio* packages are inapplicable to 2D systems. To overcome this issue, we have considered six different vacuum thicknesses and applied the effective medium theory method proposed by Freysoldt *et al.* [35] to calculate the 2D dielectric constant:

$$\begin{aligned} \varepsilon_{o,\parallel}^{\text{calc}} &= 1 + \frac{(\varepsilon_{o,\parallel}^{\text{2D}} - 1)t}{c}, \\ \frac{1}{\varepsilon_{o,\perp}^{\text{calc}}} &= 1 - \frac{(\varepsilon_{o,\perp}^{\text{2D}} - 1)t}{\varepsilon_{o,\perp}^{\text{2D}} c}, \end{aligned} \quad (1)$$

where $\varepsilon_{o,\parallel}^{\text{calc}}$ and $\varepsilon_{o,\perp}^{\text{calc}}$ are the in-plane and out-of-plane dielectric constant under vacuum distance c obtained from a single-run *ab initio* calculation, $\varepsilon_{o,\parallel}^{\text{2D}}$ and $\varepsilon_{o,\perp}^{\text{2D}}$ are the

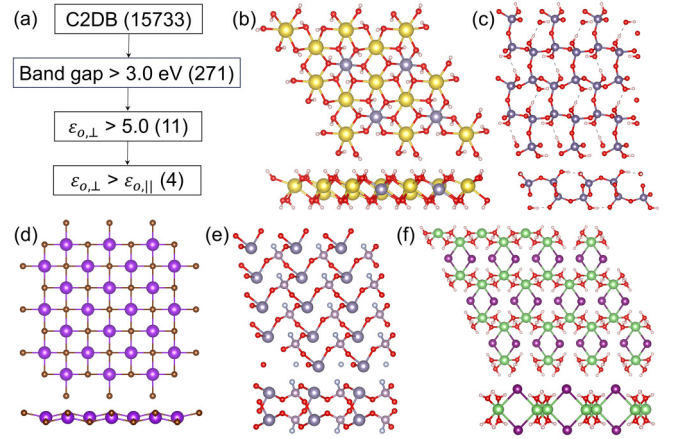


FIG. 1. (a) High-throughput screening flow of 2D dielectrics. (b)–(f) Lattice structures of the 11 candidates, both the top (upper panel) and side (lower panel) views are shown. The structures are shown using the VESTA code [34].

corresponding real dielectric constants, and t is the dielectric thickness. For anisotropic dielectrics, the average value $\varepsilon_{o,\parallel}^{\text{2D}} = 0.5(\varepsilon_x^{\text{2D}} + \varepsilon_y^{\text{2D}})$ is taken as the in-plane dielectric constant, where $\varepsilon_x^{\text{2D}}$ and $\varepsilon_y^{\text{2D}}$ are the dielectric constants along the x and y directions, respectively. Taking monolayer $\text{SnNa}_2\text{H}_6\text{O}_6$ as an example, we plot $\varepsilon_{o,\parallel}^{\text{calc}}$ and $\varepsilon_{o,\perp}^{\text{calc}}$ as a function of $1/c$ in Fig. S1 of the Supplemental Material [33]. Fitting the data, we get the slope $s_1 = 31.7$ and $s_2 = -5.57$ (note that the intercept of the two lines with the vertical axis is close to 1). It is obvious that

$$\begin{aligned} \varepsilon_{o,\parallel}^{\text{2D}} &= 1 + \frac{s_1}{t}, \\ \varepsilon_{o,\perp}^{\text{2D}} &= \frac{t}{t + s_2}. \end{aligned} \quad (2)$$

Therefore, the $\varepsilon_{o,\parallel}^{\text{2D}}$ and $\varepsilon_{o,\perp}^{\text{2D}}$ can be obtained once t is known. For 2D materials exfoliated from bulk, t can be well defined as the distance between two adjacent layers. However, most monolayers in C2DB do not have corresponding bulk materials. Here, the thickness is defined as the summation of the exact thickness (the distance between the two outer atomic planes) and the maximum vdW radius of the outer atoms.

Table S1 of the Supplemental Material [33] shows the calculated dielectric constants. It is found that 39 monolayers have relatively large $\varepsilon_{o,\parallel}^{\text{2D}}$ (> 10.0), including ZnCl_2 and ZnBr_2 . Note that our calculated values differ slightly from those in Ref. [21], which is attributed to the variations in thickness definition. However, the differences are relatively small, and the overall trend remains consistent. In general, the in-plane dielectric constant is larger than the out-of-plane. This observation is understandable since the in-plane bonding is usually stronger than the out-of-plane bonding, which may cause higher polarization in the in-plane. Considering the out-of-plane dielectric properties, we found that 11 monolayers have $\varepsilon_{o,\perp}^{\text{2D}}$ greater than 5.0, higher than the commonly used dielectrics SiO_2 , BN, and Al_2O_3 [14–16]. It indicates that those monolayers could potentially serve as better dielectrics. The lattice structures of the 11 candidates are categorized into five types, as shown in Figs. 1(b)–1(f). All these structures

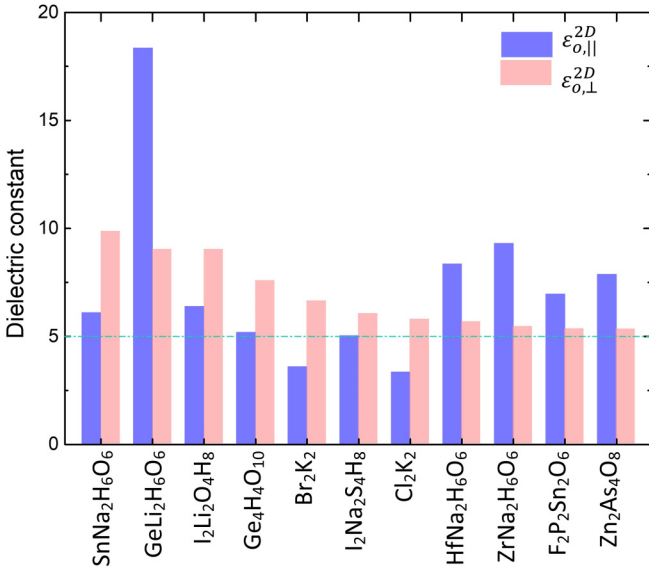


FIG. 2. Calculated in-plane dielectric constant $\epsilon_{o,||}^{2D}$ (blue) and out-of-plane dielectric constant $\epsilon_{o,\perp}^{2D}$ (red) of the 11 candidates. The green dashed line represents a dielectric constant equal to 5.0.

have light atoms distributing at the outer atomic planes, and many bonds tend to align with the out-of-plane, except for Br_2K_2 , which forms an almost planar layer.

Figure 2 shows the $\epsilon_{o,||}^{2D}$ and $\epsilon_{o,\perp}^{2D}$ of the 11 candidates with a descending $\epsilon_{o,\perp}^{2D}$. The following are found: (1) $\text{GeLi}_2\text{H}_6\text{O}_6$ has the highest $\epsilon_{o,||}^{2D}$ (18.4), which is comparable with bulk HfO_2 [36]. (2) $\text{SnNa}_2\text{H}_6\text{O}_6$ has the highest $\epsilon_{o,\perp}^{2D}$ (9.9), followed by $\text{GeLi}_2\text{H}_6\text{O}_6$ (9.0), $\text{I}_2\text{Li}_2\text{O}_4\text{H}_8$ (9.0), $\text{Ge}_4\text{H}_4\text{O}_{10}$ (7.6), etc. The $\epsilon_{o,\perp}^{2D}$ of all the 11 candidates is much higher than 2D hexagonal BN (3.0), but it is still lower than bulk HfO_2 (~ 20.0). However, HfO_2 suffers from low crystallization and poor stability, and its fabrication onto channel materials is complicated [37]. (3) The nine candidates, $\text{SnNa}_2\text{H}_6\text{O}_6$, $\text{GeLi}_2\text{H}_6\text{O}_6$, $\text{I}_2\text{Li}_2\text{O}_4\text{H}_8$, $\text{Ge}_4\text{H}_4\text{O}_{10}$, $\text{I}_2\text{Na}_2\text{S}_4\text{H}_8$, $\text{HfNa}_2\text{H}_6\text{O}_6$, $\text{ZrNa}_2\text{H}_6\text{O}_6$, $\text{F}_2\text{P}_2\text{Sn}_2\text{O}_6$, and $\text{Zn}_2\text{As}_4\text{O}_8$, have both $\epsilon_{o,||}^{2D}$ and $\epsilon_{o,\perp}^{2D}$ larger than 5.0, which is highly desirable for the recently proposed vertical FET [17–20]. (4) Four materials have higher $\epsilon_{o,\perp}^{2D}$ than $\epsilon_{o,||}^{2D}$ ($\text{SnNa}_2\text{H}_6\text{O}_6$, $\text{I}_2\text{Li}_2\text{O}_4\text{H}_8$, $\text{Ge}_4\text{H}_4\text{O}_{10}$, $\text{I}_2\text{Na}_2\text{S}_4\text{H}_8$), which is rare in 2D materials. This unusual feature is an indication that the out-of-plane bonding is stronger than that of the in-plane. We will discuss it in detail later.

It looks like most candidates have polaristic H-O (or H-S) bonds. This strong ionic feature arises from the significant difference in electronegativity between H and O (S). Moreover, the four candidates $\text{SnNa}_2\text{H}_6\text{O}_6$, $\text{GeLi}_2\text{H}_6\text{O}_6$, $\text{HfNa}_2\text{H}_6\text{O}_6$, and $\text{ZrNa}_2\text{H}_6\text{O}_6$ have the same structures and chemical formula $AB_2\text{H}_6\text{O}_6$. However, $\epsilon_{o,\perp}^{2D}$ of $\text{SnNa}_2\text{H}_6\text{O}_6$ and $\text{GeLi}_2\text{H}_6\text{O}_6$ is much higher than $\text{HfNa}_2\text{H}_6\text{O}_6$ and $\text{ZrNa}_2\text{H}_6\text{O}_6$. All four monolayers have similar highly polaristic H-O bonds. Therefore, the significant difference in dielectric constants is possibly from the A and B atoms. To get possible rules/guidelines, we picked out all $AB_2\text{H}_6\text{O}_6$ in the 271 monolayers. They are $\text{SnNa}_2\text{H}_6\text{O}_6$ (9.9), $\text{GeLi}_2\text{H}_6\text{O}_6$ (9.0), $\text{HfNa}_2\text{H}_6\text{O}_6$ (5.7), $\text{ZrNa}_2\text{H}_6\text{O}_6$ (5.4), $\text{PbK}_2\text{H}_6\text{O}_6$ (4.5), $\text{GeNa}_2\text{H}_6\text{O}_6$ (4.5), $\text{SnK}_2\text{H}_6\text{O}_6$ (4.0), and $\text{GeK}_2\text{H}_6\text{O}_6$ (3.4).

TABLE I. Calculated in-plane and out-of-plane Born effective charges Z of A atoms of the eight $AB_2\text{H}_6\text{O}_6$. The out-of-plane dielectric constant $\epsilon_{o,\perp}^{2D}$, the thickness t and the electronegativity χ_A of A atoms are also shown for comparison [38].

	$\epsilon_{o,\perp}^{2D}$	t	$Z_{ }$	Z_{\perp}	χ_A
$\text{SnNa}_2\text{H}_6\text{O}_6$	9.9	6.20	3.29	1.57	1.96
$\text{GeLi}_2\text{H}_6\text{O}_6$	9.0	5.94	3.44	1.43	2.01
$\text{HfNa}_2\text{H}_6\text{O}_6$	5.7	6.33	4.28	1.87	1.30
$\text{ZrNa}_2\text{H}_6\text{O}_6$	5.4	6.36	4.39	1.85	1.33
$\text{PbK}_2\text{H}_6\text{O}_6$	4.5	6.40	3.07	1.50	1.87
$\text{GeNa}_2\text{H}_6\text{O}_6$	4.5	6.00	3.21	1.60	2.01
$\text{SnK}_2\text{H}_6\text{O}_6$	4.0	6.40	3.15	1.65	1.96
$\text{GeK}_2\text{H}_6\text{O}_6$	3.4	6.41	3.09	1.67	2.01

The values in the parentheses represent the corresponding $\epsilon_{o,\perp}^{2D}$. By comparing their $\epsilon_{o,\perp}^{2D}$ and the Born effective charges (see Table I), we found that the A atom tends to have a large Born effective charge but not that large in high $\epsilon_{o,\perp}^{2D}$ dielectrics, indicating that the A atom has small electronegativity but not that small. This explains that the aforementioned $\text{SnNa}_2\text{H}_6\text{O}_6$ and $\text{GeLi}_2\text{H}_6\text{O}_6$ have higher dielectric constants than $\text{HfNa}_2\text{H}_6\text{O}_6$ and $\text{ZrNa}_2\text{H}_6\text{O}_6$. However, it cannot explain why $\text{GeK}_2\text{H}_6\text{O}_6$ and $\text{SnK}_2\text{H}_6\text{O}_6$ have the smallest $\epsilon_{o,\perp}^{2D}$ in the eight materials. We suspect it is related to the B atom's radius and the lattice constant. The radius of the K (243 pm) atom is much larger than Na (190 pm) and Li (167 pm), leading to the lattice constant of $\text{SnK}_2\text{H}_6\text{O}_6$ (6.62 Å) being much larger than that of $\text{SnNa}_2\text{H}_6\text{O}_6$ (5.99 Å). In addition, the thickness of $\text{SnK}_2\text{H}_6\text{O}_6$ (6.20 Å) is smaller than $\text{SnNa}_2\text{H}_6\text{O}_6$ (6.40 Å), resulting in more projection of the Na-O bond onto out-of-plane (the dihedral angle of the B-O bond with the in-plane is 39.2° for $\text{SnNa}_2\text{H}_6\text{O}_6$ and 36.6° for $\text{SnK}_2\text{H}_6\text{O}_6$). Those features lead to longer B-O bond lengths and fewer projections in the former, thus weaker bond coupling strength, resulting in smaller dielectric constants (both in-plane and out-of-plane) of $\text{SnK}_2\text{H}_6\text{O}_6$.

Besides a large dielectric constant, a suitable dielectric should have a large band offset with the channel semiconductor to minimize leakage current caused by the Schottky emission of carriers into the dielectrics. Figure 3 displays the calculated absolute conduction band minimum (CBM) and valence band maximum (VBM) with respect to the vacuum level, where the red and black lines represent the CBM and VBM. The vacuum level is set as 0 eV. Note that we have adopted the HSE method to get more reliable band gaps (see the method of the calculation of band alignment and corresponding example in the Supplemental Material [33]). It is found that all the 11 monolayers have electron affinity (here, it is the absolute value of the CBM) higher than 0.9 eV and a large band gap in the range 4.9–6.1 eV (denoted by the cyan areas in Fig. 3). The CBM of the common experimentally studied 2D semiconductors, i.e., monolayer MoS_2 , WS_2 , MoSe_2 , and black phosphorene are -4.27 , -3.96 , -3.90 , and -3.91 eV respectively [39,40]. If those 2D semiconductors are taken as the channel in *n*-type FETs, except $\text{Ge}_4\text{H}_4\text{O}_{10}$, all the other candidates are promising 2D dielectrics.

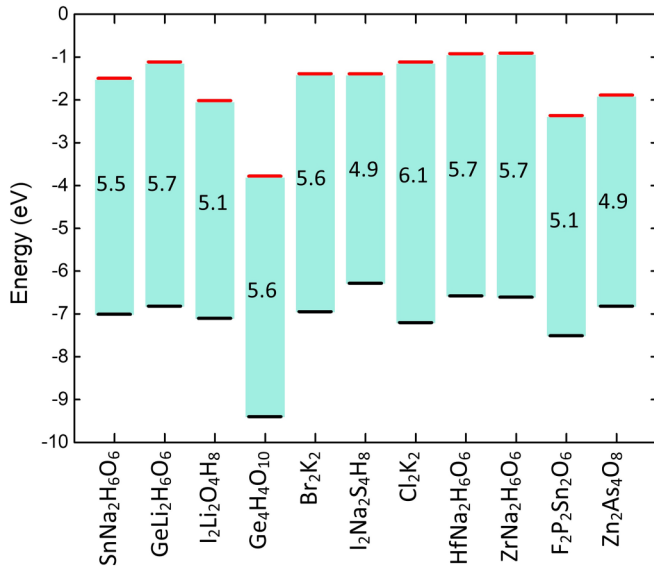


FIG. 3. Calculated band alignments of the 11 candidates. The conduction band minimum and the valance band maximum are indicated by the red and black lines. The vacuum level is 0 eV. The band gap is shown in the cyan area. The values are calculated using the HSE method.

As mentioned above, four materials have larger $\epsilon_{o,\perp}^{2D}$ than $\epsilon_{o,\parallel}^{2D}$. We suspect it is because the out-of-plane bonding is stronger than the in-plane, which is rare in 2D materials. Indeed, that is confirmed by the electron localization function (ELF), as shown in Fig. 4. Figures 4(a)–4(c) show the sliced

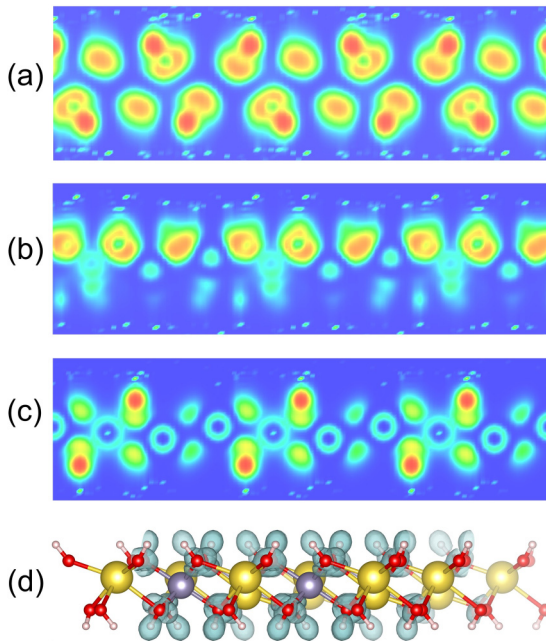


FIG. 4. (a)–(c) The sliced electron localization function of $\text{SnNa}_2\text{H}_6\text{O}_6$ along the (110) plane using a 3×3 supercell with different distances from the origin: (a) 7.5 Å, (b) 8.0 Å, and (c) 9.0 Å, respectively. (d) The electron localization function of $\text{SnNa}_2\text{H}_6\text{O}_6$ with an isosurface value of $0.8e$.

ELF of $\text{SnNa}_2\text{H}_6\text{O}_6$ along the (110) plane using a 3×3 supercell with different distances from the origin: (a) 7.5 Å from the origin: this represents the center between the two (110) planes where the Na atoms locate; (b) 8.0 Å from the origin: the oxygen atoms are at this plane; (c) 9.0 Å from the origin: the Na and Sn atoms are at this plane. The three-sliced diagrams show that electrons always tend to be located around O and H atoms, while there is almost no electron distribution around Na and Sn atoms. Figure 4(d) shows the ELF with an isosurface value of $0.8e$. The electrons mainly localize around the H-O bond, confirming the stronger bond strength. Furthermore, the electron density expands significantly along out-of-plane, indicating that the bond strength is quite strong. Considering that the H-O bond is rather polaristic, those features result in a relatively high dielectric constant along out-of-plane. From the above analysis, we gain a general rule for quickly accessing good 2D dielectrics based on the structural properties and electronegativity table of elements: Searching for high-performance 2D dielectrics is to find materials with bonds along out-of-plane that are highly ionic, which means the atoms forming those bonds have high electronegativity differences.

IV. SUMMARY

In summary, we have studied the dielectric properties of 271 stable monolayers in the C2DB using high-throughput first-principles calculations. It is found that 11 monolayers show an out-of-plane dielectric constant over 5.0, which is highly desirable for 2D dielectrics. Moreover, four monolayers show a larger out-of-plane dielectric constant than in-plane, which is rare in 2D materials. We uncovered that this unusual feature is related to the stronger bonding strength in the out-of-plane. Combining with the band alignments, we identify ten monolayers, including $\text{SnNa}_2\text{H}_6\text{O}_6$, $\text{GeLi}_2\text{H}_6\text{O}_6$, $\text{HfNa}_2\text{H}_6\text{O}_6$, and $\text{ZrNa}_2\text{H}_6\text{O}_6$, etc., that can serve as good 2D dielectrics if MoS_2 is the channel. Our work not only discovers several potential 2D dielectrics, but also uncovers the underlying physics that leads to the large out-of-plane dielectrics in 2D materials, and offers a general guideline to quickly access suitable dielectrics from their structures and electronegativity table. Searching for high-performance 2D dielectrics is finding materials with bonds along out-of-plane that are highly ionic, which means the atoms forming those bonds have high electronegativity differences.

The data that support the findings of this study are available from the corresponding author upon reasonable request.

ACKNOWLEDGMENTS

This work was supported by the National Natural Science Foundation of China (Grant No. 12104143), Natural Science Foundation of Hunan Province (Grants No. 2022JJ40027 and No. 2022JJ40028), and Fundamental Research Funds for the Central Universities (Grants No. 531118010595 and No. 531118010619).

The authors declare that they have no known competing financial interests or personal relationships that could have appeared to influence the work reported in this paper.

- [1] B. Radisavljevic, A. Radenovic, J. Brivio, V. Giacometti, and A. Kis, Single-layer MoS₂ transistors, *Nat. Nanotechnol.* **6**, 147 (2011).
- [2] O. Lopez-Sanchez, D. Lembke, M. Kayci, A. Radenovic, and A. Kis, Ultrasensitive photodetectors based on monolayer MoS₂, *Nat. Nanotechnol.* **8**, 497 (2013).
- [3] L. Li, Y. Yu, G. J. Ye, Q. Ge, X. Ou, H. Wu, D. Feng, X. H. Chen, and Y. Zhang, Black phosphorus field-effect transistors, *Nat. Nanotechnol.* **9**, 372 (2014).
- [4] T. Roy, M. Tosun, J. S. Kang, A. B. Sachid, S. B. Desai, M. Hettick, C. C. Hu, and A. Javey, Field-effect transistors built from all two-dimensional material components, *ACS Nano* **8**, 6259 (2014).
- [5] M. Chhowalla, D. Jena, and H. Zhang, Two-dimensional semiconductors for transistors, *Nat. Rev. Mater.* **1**, 16052 (2016).
- [6] G. Fiori, F. Bonaccorso, G. Iannaccone, T. Palacios, D. Neumaier, A. Seabaugh, S. K. Banerjee, and L. Colombo, Electronics based on two-dimensional materials, *Nat. Nanotechnol.* **9**, 768 (2014).
- [7] Y. Liu, X. Duan, H.-J. Shin, S. Park, Y. Huang, and X. Duan, Promises and prospects of two-dimensional transistors, *Nature (London)* **591**, 43 (2021).
- [8] Y. Du, H. Liu, A. T. Neal, M. Si, and P. D. Ye, Molecular doping of multilayer MoS₂ field-effect transistors: Reduction in sheet and contact resistances, *IEEE Electron Device Lett.* **34**, 1328 (2013).
- [9] J. L. Wang, Q. Yao, C. W. Huang, X. M. Zou, L. Liao, S. S. Chen, Z. Y. Fan, K. Zhang, W. Wu, X. H. Xiao *et al.*, High mobility MoS₂ transistor with low Schottky barrier contact by using atomic thick h-BN as a tunneling layer, *Adv. Mater.* **28**, 8302 (2016).
- [10] L. Cheng, C. M. Zhang, and Y. Y. Liu, Why two-dimensional semiconductors generally have low electron mobility, *Phys. Rev. Lett.* **125**, 177701 (2020).
- [11] L. Cheng, C. Zhang, and Y. Liu, The optimal electronic structure for high-mobility 2D semiconductors: Exceptionally high hole mobility in 2D antimony, *J. Am. Chem. Soc.* **141**, 16296 (2019).
- [12] L. Cheng and C. H. Li, Searching for high-performance two-dimensional channel materials from first-principles calculations, *J. Phys. Chem. C* **126**, 21149 (2022).
- [13] L. Cheng, C. Zhang, and Y. Liu, Intrinsic charge carrier mobility of 2D semiconductors, *Comput. Mater. Sci.* **194**, 110468 (2021).
- [14] M. L. Green, E. P. Gusev, R. Degraeve, and E. L. Garfunkel, Ultrathin (<4 nm) SiO₂ and Si-O-N gate dielectric layers for silicon microelectronics: Understanding the processing, structure, and physical and electrical limits, *J. Appl. Phys.* **90**, 2057 (2001).
- [15] Z. Wang, L. Wei, S. Wang, T. Wu, L. Sun, C. Ma, X. Tao, and S. Wang, 2D SiP₂/h-BN for a gate-controlled phototransistor with ultrahigh sensitivity, *ACS Appl. Mater. Interfaces* **15**, 15810 (2023).
- [16] M. Geiger, M. Hagel, T. Reindl, J. Weis, R. T. Weitz, H. Solodenko, G. Schmitz, U. Zschieschang, H. Klauk, and R. Acharya, Optimizing the plasma oxidation of aluminum gate electrodes for ultrathin gate oxides in organic transistors, *Sci. Rep.* **11**, 6382 (2021).
- [17] L. Liu, L. Kong, Q. Li, C. He, L. Ren, Q. Tao, X. Yang, J. Lin, B. Zhao, Z. Li *et al.*, Transferred van der Waals metal electrodes for sub-1-nm MoS₂ vertical transistors, *Nat. Electron.* **4**, 342 (2021).
- [18] Y. Liu, Y. Huang, and X. Duan, Van der Waals integration before and beyond two-dimensional materials, *Nature (London)* **567**, 323 (2019).
- [19] Y. Liu, N. O. Weiss, X. Duan, H.-C. Cheng, Y. Huang, and X. Duan, Van der Waals heterostructures and devices, *Nat. Rev. Mater.* **1**, 16042 (2016).
- [20] T. Georgiou, R. Jalil, B. D. Belle, L. Britnell, R. V. Gorbachev, S. V. Morozov, Y.-J. Kim, A. Gholinia, S. J. Haigh, O. Makarovskiy *et al.*, Vertical field-effect transistor based on graphene-WSe₂ heterostructures for flexible and transparent electronics, *Nat. Nanotechnol.* **8**, 100 (2013).
- [21] M. R. Osanloo, M. L. Van de Put, A. Saadat, and W. G. Vandenberghe, Identification of two-dimensional layered dielectrics from first principles, *Nat. Commun.* **12**, 5051 (2021).
- [22] B. Zhang, Y. Zhu, Y. Zeng, Z. Zhao, X. Huang, D. Qiu, Z. Fang, J. Wang, J. Xu, R. Wang *et al.*, General approach for two-dimensional rare-earth oxyhalides with high gate dielectric performance, *J. Am. Chem. Soc.* **145**, 11074 (2023).
- [23] S. Haastrup, M. Strange, M. Pandey, T. Deilmann, P. S. Schmidt, N. F. Hinsche, M. N. Gjerding, D. Torelli, P. M. Larsen, A. C. Riis-Jensen *et al.*, The computational 2D materials database: high-throughput modeling and discovery of atomically thin crystals, *2D Mater.* **5**, 042002 (2018).
- [24] M. N. Gjerding, A. Taghizadeh, A. Rasmussen, S. Ali, F. Bertoldo, T. Deilmann, U. P. Holguin, N. R. Knsgaard, M. Kruse, A. H. Larsen *et al.*, Recent progress of the computational 2D materials database (C2DB), *2D Mater.* **8**, 044002 (2021).
- [25] G. Kresse and J. Hafner, *Ab initio* molecular dynamics for liquid metals, *Phys. Rev. B* **47**, 558 (1993).
- [26] G. Kresse and J. Hafner, *Ab initio* molecular-dynamics simulation of the liquid-metal-amorphous-semiconductor transition in germanium, *Phys. Rev. B* **49**, 14251 (1994).
- [27] G. Kresse and J. Furthmüller, Efficiency of *ab-initio* total energy calculations for metals and semiconductors using a plane-wave basis set, *Comput. Mater. Sci.* **6**, 15 (1996).
- [28] P. E. Blöchl, Projector augmented-wave method, *Phys. Rev. B* **50**, 17953 (1994).
- [29] J. P. Perdew, K. Burke, and M. Ernzerhof, Generalized gradient approximation made simple, *Phys. Rev. Lett.* **77**, 3865 (1996).
- [30] J. P. Perdew, K. Burke, and Y. Wang, Generalized gradient approximation for the exchange-correlation hole of a many-electron system, *Phys. Rev. B* **54**, 16533 (1996).
- [31] J. Heyd, G. E. Scuseria, and M. Ernzerhof, Hybrid functionals based on a screened Coulomb potential, *J. Chem. Phys.* **118**, 8207 (2003).
- [32] J. Heyd, G. E. Scuseria, and M. Ernzerhof, Erratum: "Hybrid functionals based on a screened Coulomb potential" [J. Chem. Phys. **118**, 8207 (2003)], *J. Chem. Phys.* **124**, 219906 (2006).
- [33] See Supplemental Material at <http://link.aps.org/supplemental/10.1103/PhysRevB.108.235409> for calculated dielectric constants as a function of the inverse of vacuum thickness for monolayer SnNa₂H₆O₆, method on the calculation of band alignment, and dielectric constants of all the monolayers considered.
- [34] K. Momma and F. Izumi, VESTA 3 for three-dimensional visualization of crystal, volumetric and morphology data, *J. Appl. Crystallogr.* **44**, 1272 (2011).

- [35] C. Freysoldt, P. Eggert, P. Rinke, A. Schindlmayr, and M. Scheffler, Screening in two dimensions: GW calculations for surfaces and thin films using the repeated-slab approach, *Phys. Rev. B* **77**, 235428 (2008).
- [36] D. Banerjee, R. Sewak, C. C. Dey, D. Toprek, and P. K. Pujari, Orthorhombic phases in bulk pure HfO₂: Experimental observation from perturbed angular correlation spectroscopy, *Mater. Today: Commun.* **26**, 101827 (2021).
- [37] S. Tongpeng, K. Makbun, P. Peanporm, R. Sangkorn, O. Namsar, P. Janphuang, S. Pojprapai, and S. Jainsirisomboon, Fabrication characterization of hafnium oxide thin films, *Mater. Today: Proc.* **17**, 1555 (2019).
- [38] L. Pauling, The nature of the chemical bond iv. the energy of single bonds and the relative electronegativity of atoms, *J. Am. Chem. Soc.* **54**, 3570 (1932).
- [39] C. Gong, H. Zhang, W. Wang, L. Colombo, R. M. Wallace, and K. Cho, Band alignment of two-dimensional transition metal dichalcogenides: Application in tunnel field effect transistors, *Appl. Phys. Lett.* **103**, 053513 (2013).
- [40] Y. Cai, G. Zhang, and Y.-W. Zhang, Layer-dependent band alignment and work function of few-layer phosphorene, *Sci. Rep.* **4**, 6677 (2014).